A PARAMETRIZATION OF THE CONVECTIVE ATMOSPHERIC BOUNDARY LAYER AND ITS APPLICATION INTO A GLOBAL CLIMATE MODEL

A.A.M. Holtslag
Royal Netherlands Meteorological Institute (KNMI), De Bilt, The Netherlands

B.A. Boville, C.-H. Moeng
National Center for Atmospheric Research (NCAR), Boulder, USA

Abstract: In this paper we focus on vertical diffusion of heat and passive scalars (like moisture) in the convective atmospheric boundary layer. In the first part of the paper, a summary of the recent work by Holtslag and Moeng (1991) is given. In this work the heat and scalar flux equations are analyzed with data obtained from large-eddy-simulations. The findings can be used in a modified flux-gradient approach, which takes account for nonlocal convective vertical exchange utilizing so-called counter-gradient transport and a nonlocal diffusivity coefficient. In the second part of the paper, the previous findings are simplified and applied in the latest version of the NCAR community climate model (CCM2). The impact of the nonlocal approach is illustrated in comparison with the usual local diffusion approach (Holtslag and Boville, 1992).

1. INTRODUCTION

Turbulence in the atmospheric boundary layer (ABL) results in mixing of heat, moisture, momentum, and passive scalars. Global weather forecasting and climate models typically describe the turbulent mixing with an eddy diffusivity based on local gradients of wind and potential temperature. Such a so-called "local K" approach, is discussed for instance by Louis (1979). Local K-theory may fail in the unstable boundary layer because the influence of large eddy transports is not accounted for (e.g., Wyngaard and Brost 1984; Ebert et al 1989; Holtslag and Moeng 1991). This will affect the profiles of mean quantities, especially at locations where dry convection is of importance in the ABL. Moreover, in the upper half of the convective, atmospheric boundary layer (CABL), the upward transport of heat is typically accompanied by a slightly stable temperature gradient indicating counter-gradient transport.

Deardorff (1972) derived a counter-gradient term for heat in the CABL by neglecting the transport term in the heat-flux equation. Holtslag and Moeng (1991, hereafter HM91) derived a modified counter-gradient term by utilizing the recent results of large-eddy simulations (LES) by Moeng and Wyngaard (1989). HM91 introduced an empirical parameterization for the transport term in the heat-flux equation and used the modified Rotta return-to-

isotropy hypothesis by Moeng and Wyngaard (1986). This leads directly to a simple description of vertical heat transport. In section 2 we compare these results with those of Deardorff.

A similar analysis as for heat diffusion can be given for *top-down/bottom-up diffusion* (Wyngaard and Brost 1984). With such an approach, the impact on the diffusion of scalar fluxes at the surface and at the top of the CABL are distinguished. In previous studies it has been found that the eddy diffusivity of the *bottom-up* diffusion has a singularity in the mid-part of the CABL, while the *top-down* diffusivity is well-behaved (Moeng and Wyngaard 1984; Wyngaard 1987; Schumann 1989). Using a counter-gradient correction for the bottom-up diffusion of a scalar similar to the one for heat, we obtain a well-behaved diffusivity for the bottom-up field. Consequently, the findings can be generalized for the transport of any scalar, such as the specific humidity (q) or any other conservative species (C).

In section 3 the findings for heat and scalar diffusion are simplified and applied in the latest version of the Community Climate Model (CCM2). Since the present proposals reflect diffusion and countergradient transport in the convective boundary layer, it is referred to as *nonlocal* diffusion. For stable and neutral conditions also a nonlocal diffusivity is used, which follows the work by Troen and Mahrt (1986), and Holtslag et al (1990). In section 3 we compare the outputs of the nonlocal scheme with the usual local down-gradient diffusion approach. This work will be described in more detail in Holtslag and Boville (1992, hereafter HB92). Finally, section 4 summarizes this paper and provides conclusions.

2. NONLOCAL DIFFUSION

2.1 The heat – flux equation

Under horizontally-homogeneous conditions, the equation for the heat flux, $\overline{w\theta}$, reads in the Boussinesq approximation as (e.g., Deardorff 1972)

$$\frac{\partial \overline{w\theta}}{\partial t} = -\frac{\partial \overline{w^2\theta}}{\partial z} - \overline{w^2}\frac{\partial \Theta}{\partial z} + \beta g \overline{\theta^2} - \frac{1}{\rho_0}\overline{\theta \frac{\partial p}{\partial z}}\,, \qquad (1)$$

where θ is the potential temperature fluctuation, Θ is the mean value of the potential temperature, w is the vertical-velocity fluctuation, z is height, βg is the buoyancy parameter, ρ_0 is density of air at the reference state, p is the pressure fluctuation, and overbars denote ensemble averages. The terms on the right-hand-side (rhs) of (1) are, in order, the turbulent transport term (denoted below by T), the mean-gradient production (M), the buoyant production (B), and the pressure covariance (P). Here we have included the minus signs in the definitions of T, M and P.

Figure 1, adopted from Moeng and Wyngaard (1989), shows the vertical profiles of the terms at the rhs of (1). The terms are normalized with the height of the CABL, z_i, the convective velocity scale, w_*, and the convective temperature scale, θ_*, where

$$w_* \equiv (\beta g \overline{w\theta_0} z_i)^{1/3} , \tag{2}$$

$$\theta_* \equiv \frac{\overline{w\theta_0}}{w_*} , \tag{3}$$

and $\overline{w\theta_0}$ is the kinematic surface heat flux. The statistics shown here are from (96)[3], wave-cutoff filtered simulations over a 5 km × 5 km × 2 km numerical domain. They are averaged over the horizontal plane and over about three large-eddy-turnover-times z_i/w_*. In the LES we have $\overline{w\theta_0} \simeq 0.24$ mK/s, $z_i \simeq 1000$ m, $w_* \simeq 2$ m/s, $\theta_* \simeq 0.12$ K, and the friction velocity $u_* \simeq 0.6$ m/s.

The transport term T of (1) is not small in comparison with the other terms. In many cases (i.e., Deardorff 1972), however, this term is neglected . In second-order closure modeling, T is often modeled with the down-gradient diffusion assumption, but the latter is inappropriate owing to the dominant buoyancy effect (Moeng and Wyngaard 1989). The mean gradient term M changes sign in the mid CABL, where the buoyancy flux $\overline{w\theta}$ is positive, indicating the counter-gradient transport.

Figure 1 suggests that T is larger than P by a nearly constant value throughout most of the CABL (i.e., $0.1 \leq z/z_i \leq 0.8$). Therefore, HM91 paramerized the transport term T as

$$T \simeq P + b\frac{{w_*}^2\theta_*}{z_i} , \tag{4}$$

where $b \simeq 2$. Lenschow et al (1980; their Fig. 17) and Adrian et al (1986; their Fig. 19) provide experimental data on T and P, which can be used for comparison. We have to realize, however, that both T and P are very hard to measure due to sampling problems. Moreover, in the cited studies the pressure term P is obtained as a residual, which makes the outcome very sensitive to measuring errors. Nevertheless, T as obtained by Lenschow et al and Adrian et al, is qualitatively similar to T in Figure 1.

The pressure covariance term P is modeled as (e.g., Crow 1968; Moeng and Wyngaard 1986)

$$P \equiv -\frac{1}{\rho_0}\overline{\theta\frac{\partial p}{\partial z}} = -a\beta g\overline{\theta^2} - \frac{\overline{w\theta}}{\tau} , \tag{5}$$

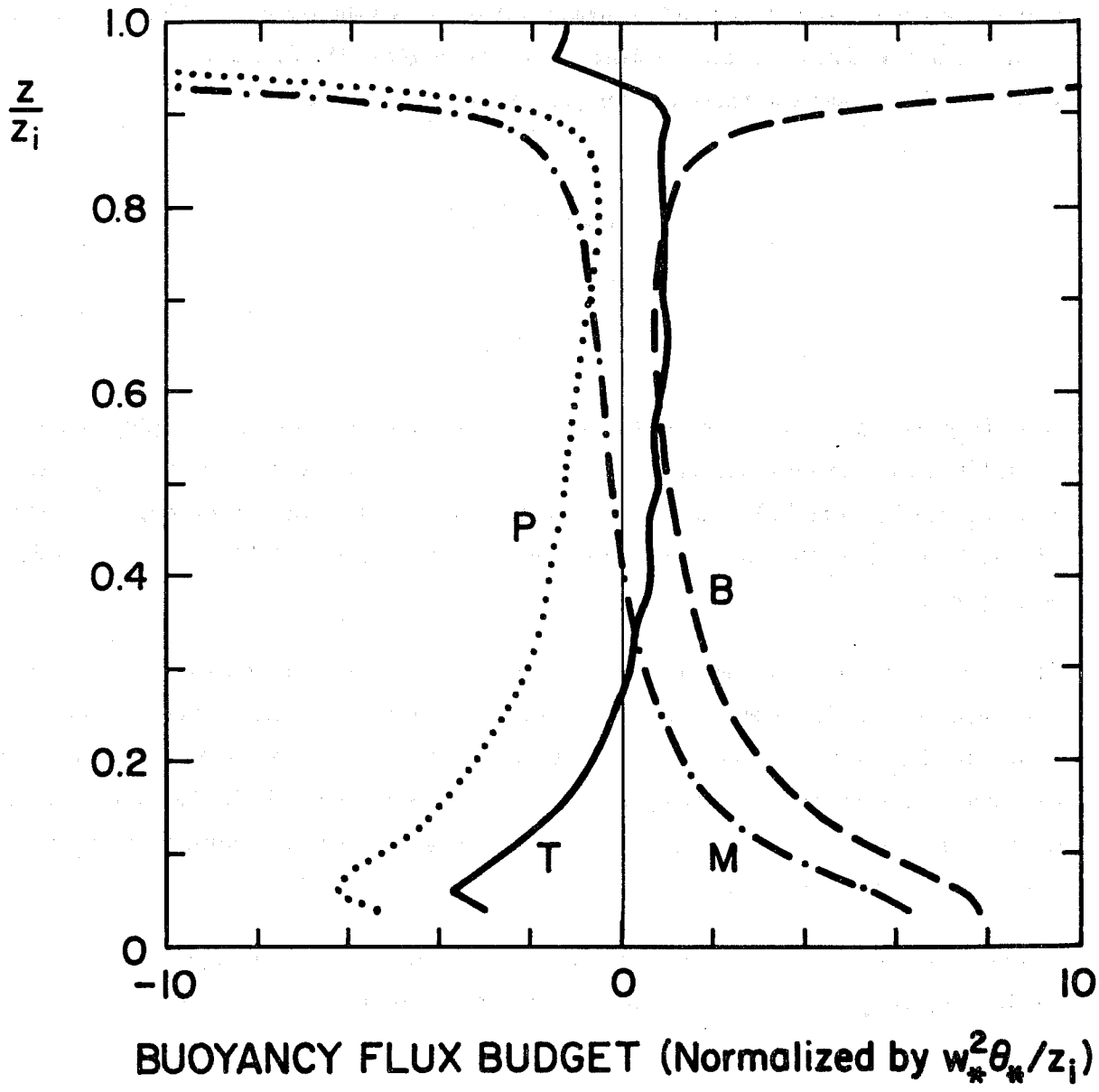

Figure 1. The normalized terms at the rhs of the heat-flux equation (1), as a function of relative height (adopted from Moeng and Wyngaard 1989). The terms are defined in the text of section 2.1.

where τ is a return-to-isotropy time scale, and a is a constant. For isotropic turbulence, $a = 1/3$. For turbulence within the CABL, Moeng and Wyngaard (1986) obtained $a \simeq 1/2$. Above the mixed-layer, a may depend on the stability and structure of the inversion layer. Often, only the second term on the rhs of (5) is taken into account; it is known as the Rotta return-to-isotropy hypothesis. The first term on the rhs of (5) shows that P is directly related to the buoyant production rate $\beta g\overline{\theta^2}$.

When (4) and (5) are substituted into (1), we obtain

$$\frac{\partial \overline{w\theta}}{\partial t} = -\overline{w^2}\frac{\partial \Theta}{\partial z} + (1-2a)\beta g\overline{\theta^2} - 2\frac{\overline{w\theta}}{\tau} + \frac{bw_*^2\theta_*}{z_i} . \tag{6}$$

By adopting $a = 1/2$ of Moeng and Wyngaard (1986), the buoyant production term $\beta g\overline{\theta^2}$ disappears from (6). Then, in quasi-steady states, (6) becomes

$$\overline{w\theta} \simeq -\frac{\overline{w^2}}{2}\frac{\partial \Theta}{\partial z} + \frac{b}{2}\frac{w_*^2\theta_*}{z_i} . \tag{7}$$

For $a \neq 1/2$ we obtain an additional term at the rhs of (7) which is given by $(1/2-a)\beta g\overline{\theta^2}$. In such cases the description for the heat flux is no longer as simple as we present here. Therefore (7) is restricted to turbulence within the CABL for which $a \simeq 1/2$.

Although (7) is partly based on the simple empirical parameterization of (4), it is physically appealing. It shows that the heat flux depends on a local down-gradient transport (first term on the rhs) and a non-local convective transport (second term on rhs). Therefore, the form of (7) is closely related to the original proposal by Priestley and Swinbank (1947), who found from mixing-length arguments that the heat-flux expression should contain a convective part in addition to the usual down-gradient part. We note that the convective part of (7) arises from the turbulent transport term and that it is proportional to the surface heat flux $w_*\theta_*$ (see (3)). Recently, Wyngaard and Weil (1991) obtained a very similar result as (7) through a kinematic derivation. Comparison of their findings with (7) suggests that the parameter b is proportional to the skewness S of the vertical turbulent velocity field ($S = \overline{w^3}/\overline{w^2}^{3/2}$). In the CABL the skewness is positive due to fast rising updrafts and slow descending downdrafts. In the absence of skewness (e.g., $b = 0$), it is seen that (7) reduces to the usual down-gradient diffusion concept.

2.2 Eddy diffusivities and countergradient terms

To facilitate a comparison with the previous results by Deardorff (1966,1972), it is convenient to write (7) as

$$\overline{w\theta} = -K_H\left(\frac{\partial \Theta}{\partial z} - \gamma_\theta\right) , \tag{8}$$

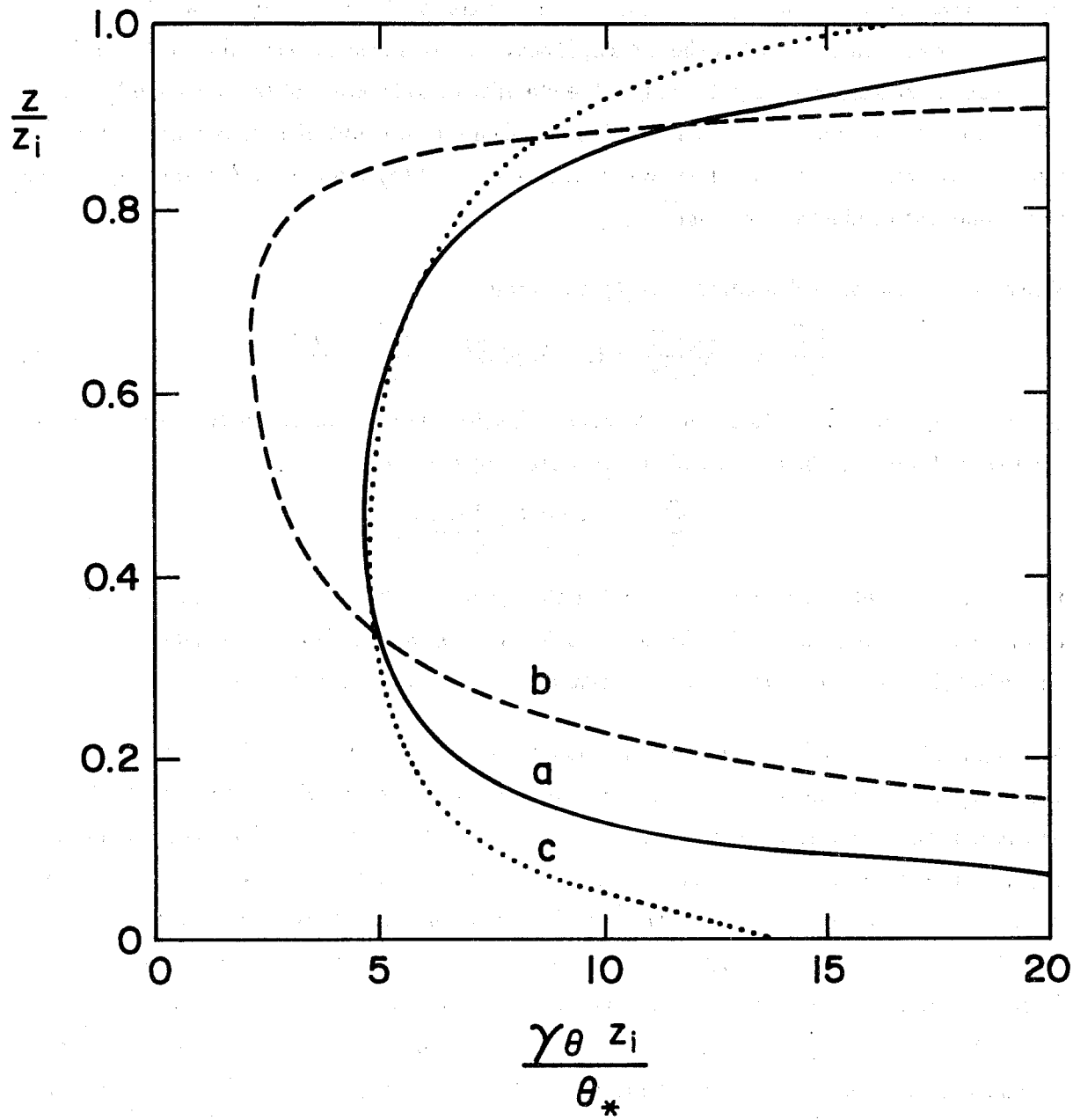

Figure 2. Plot of the non-dimensional counter-gradient term for heat, according to *a*: (9b), *b*: (10b), and *c*: as *a* but with subgrid scale contributions.

where in this case K_H and γ_θ are given by

$$K_H = \overline{w^2}\frac{\tau}{2} , \tag{9a}$$

and

$$\gamma_\theta = b\frac{w_*^2\theta_*}{\overline{w^2}z_i} . \tag{9b}$$

Here K_H and γ_θ can be interpreted as an eddy diffusivity and a counter-gradient term, respectively.

Deardorff (1972) obtained (8) by neglecting the transport term T in the heat-flux equation (1) and using (5) with $a = 0$. This means that he makes use of $P \equiv -\overline{w\theta}/\tau_D$, where τ_D is a time scale related to the turbulence energy and a mixing length. In that case, K_H and γ_θ are given by

$$K_H = \overline{w^2}\tau_D \tag{10a}$$

and

$$\gamma_\theta = \beta g\frac{\overline{\theta^2}}{\overline{w^2}} . \tag{10b}$$

The physical interpretation of the counter-gradient terms by (9b) and (10b) is very different. Equation (10b) comes from the buoyancy production term, while (9b) arises from the turbulent transport term by (4). We note that in Deardorff's (1966) paper a proper discussion of γ_θ in terms of the transport term in the *temperature variance equation* is given (see also Schumann 1987). We show here that the third-moment transport term in the ***heat-flux equation*** is also responsible for the counter-gradient term.

In Fig. 2, we compare the magnitudes of (9b) and (10b), where we have normalized γ_θ with θ_*/z_i and where all the turbulent quantities are obtained from the (resolved) LES data of Moeng and Wyngaard (1989). It is seen that the magnitude of the two expressions differs by a factor of the two near $z/z_i \simeq 0.7$ (or even more for $z/z_i < 0.2$), but that their general behavior is very similar despite the different physics (Although, strictly speaking, our results on basis of (4) apply only for $0.1 \leq z/z_i \leq 0.8$, we have extended the range in figures 3 and 4 below for illustration purposes).

Figure 3 shows a comparison of the (normalized) eddy diffusivity obtained from (8) as

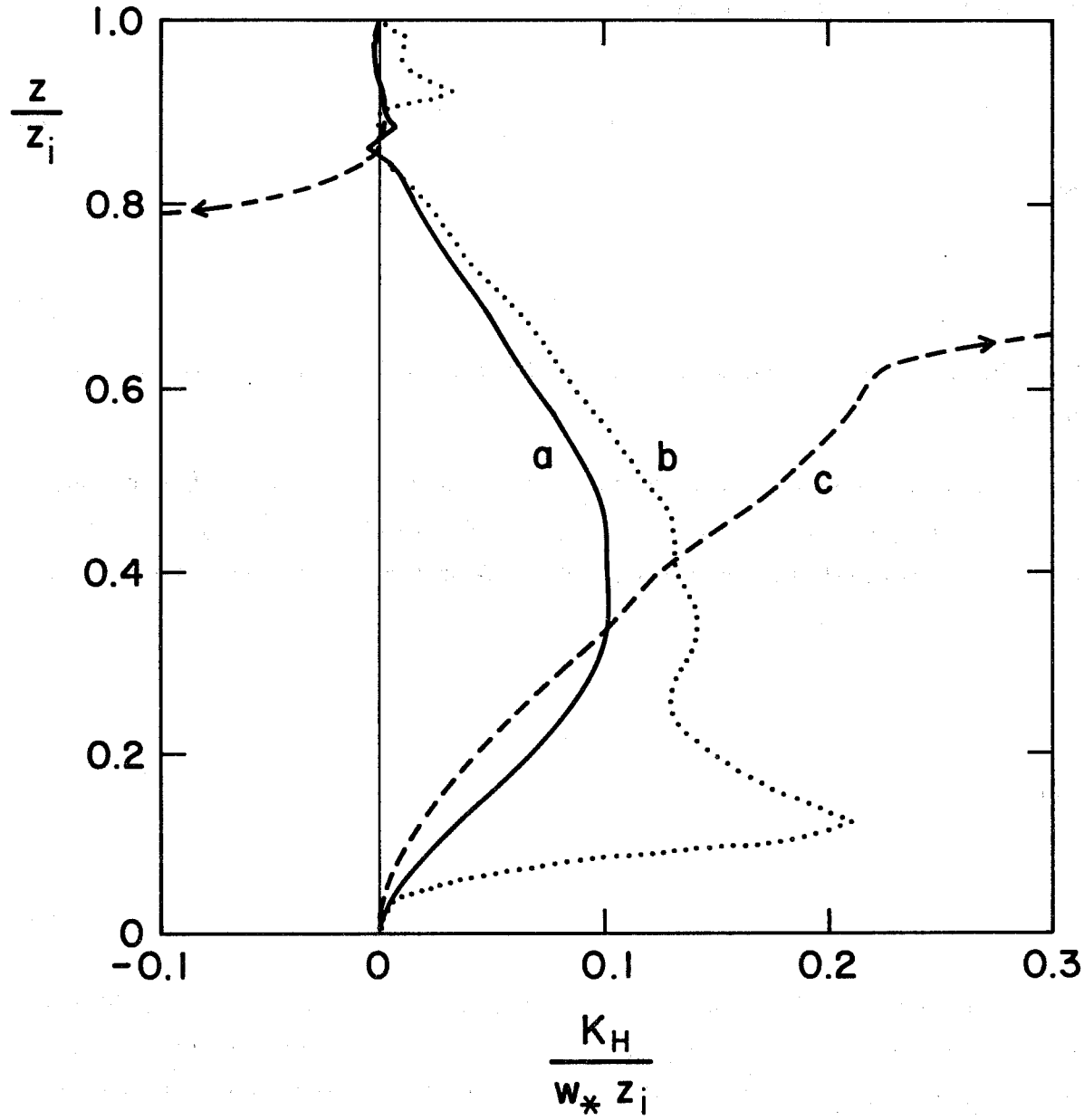

Figure 3. Plot of the non-dimensional eddy diffusivity for heat, according to *a*: (11) with (9b), *b*: (9a), and *c*: (11) with (10b).

$$\frac{K_H}{w_* z_i} = \frac{-\overline{w\theta}/\overline{w\theta_0}}{(\partial\Theta/\partial z - \gamma_\theta) z_i/\theta_*}, \tag{11}$$

utilizing the LES data for $\partial\Theta/\partial z$, $\overline{w\theta}$ (both resolved and subgrid contributions), and using (9b) for γ_θ (see curve *a*). Also, the result of (9a) is given for comparison (curve *b*), where τ is directly calculated from the *turbulence-turbulence* component of the pressure fluctuations in the LES data (see Moeng and Wyngaard 1986). It is seen that the magnitudes of the K_H values by both calculations are of the order of 0.1 in the mid part of the ABL. The result by (9a) shows an unexpected peak near $z/z_i \simeq 0.1$, that is probably due to uncertainties in the calculation of τ near that height. Overall, Fig. 3 shows that (9a) is fairly consistent with the results of (11) and (9b).

In Fig. 3 (curve *c*), we also show the result of K_H that is obtained from (11) with Deardorff's expression of γ_θ given by (10b). It is seen that a singularity appears near $z/z_i \simeq 0.7$, showing that the counter-gradient correction by (10b) is not sufficient to obtain a well behaved profile for K_H (see also Fig. 2). From the curves a & b of Fig. 3 we note that the maximum value of K_H is approximately given by $0.1 w_* z_i$. A curve fit to K_H is given as (HM91)

$$\frac{K_H}{w_* z_i} = \left(\frac{z}{z_i}\right)^{4/3} \left(1 - \frac{z}{z_i}\right)^2 \left(1 + R_H \frac{z}{z_i}\right) \tag{12}$$

for $0 \leq z/z_i \leq 1$. Here R_H is the ratio of entrainment flux to the surface flux for heat. In the LES data we have $R_H = -0.2$. Note that (12) obeys the free-convection limit in the surface layer, e.g., $K_H \propto z^{4/3}$ for small z/z_i (e.g., Panofsky and Dutton 1984). In (12), we have neglected the small contribution of shear production for simplicity. This means that (12) is limited to convective cases for which $-z_i/L \geq 5$ or $u_*/w_* \leq 0.43$ (Holtslag and Nieuwstadt 1986). It can be shown that (12) matches with the results of surface layer theory at the top of the surface layer (see HM91).

2.3 Scalar transport

To study the diffusion of scalars in a convective boundary layer, it is useful to consider so-called *top-down* and *bottom-up* scalars (Wyngaard and Brost 1984; Moeng and Wyngaard 1984; 1989). Here top-down diffusion is driven by the entrainment flux of the scalar, with a zero flux for the scalar at the surface; and the bottom-up diffusion is driven by the surface flux, with a zero entrainment flux for the scalar involved. Similarly with (8), we write for the bottom-up case

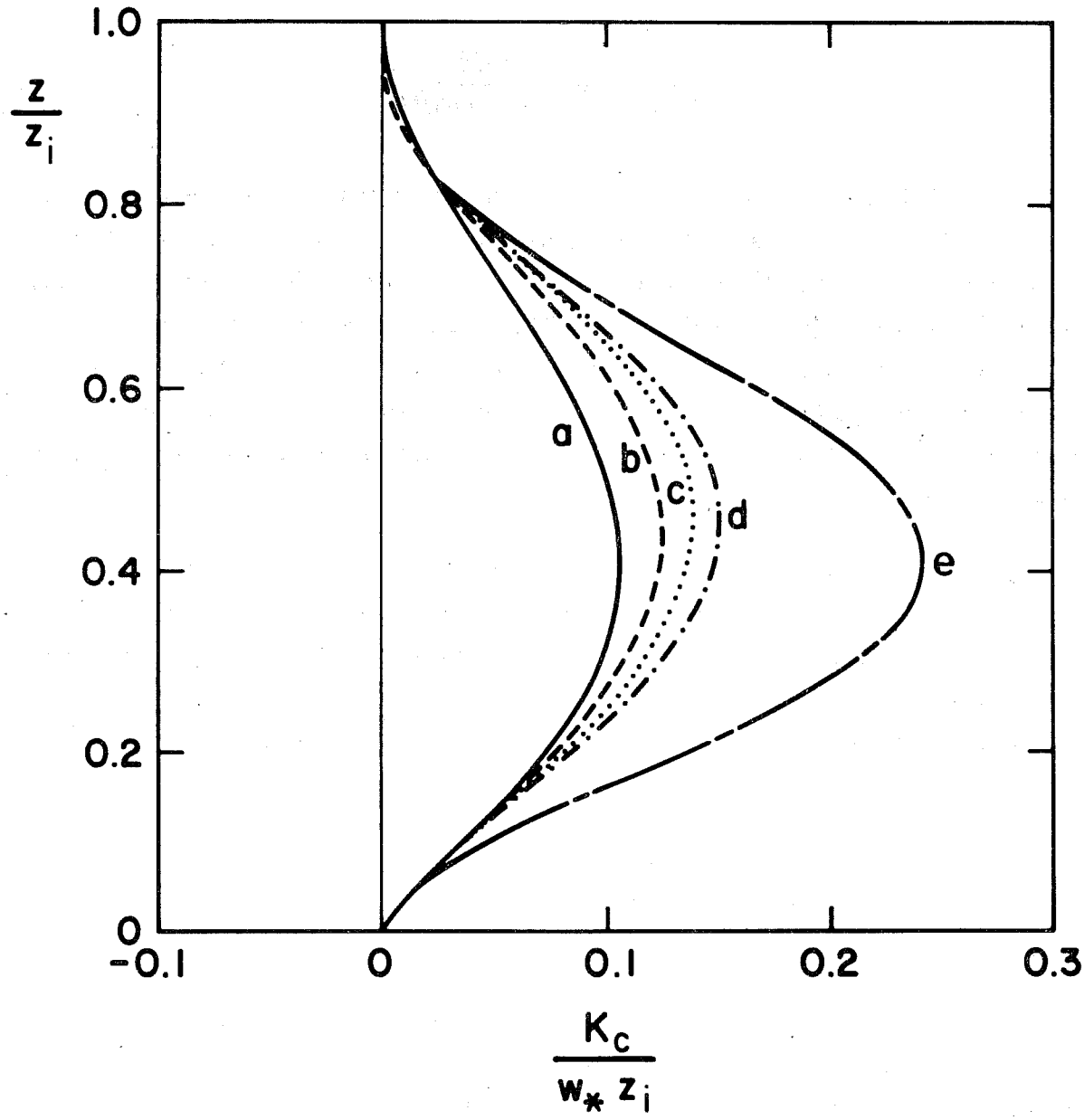

Figure 4. Plot of the non-dimensional eddy diffusivity for scalar transport by (17) with (15 a & b), for varying values of the entrainment-surface flux ratio R_c, namely *a*: 0, *b*: 0.5, *c*: 1, *d*: 1.5, *e*: ∞.

$$\overline{wc_b} = -K_b \left(\frac{\partial C_b}{\partial z} - \gamma_b \right) , \tag{13a}$$

and for the top-down case

$$\overline{wc_t} = -K_t \left(\frac{\partial C_t}{\partial z} - \gamma_t \right) , \tag{13b}$$

where in analogy with (9b) we write

$$\gamma_b = b_b \frac{w_* \overline{wc}_0}{\overline{w^2} z_i} \tag{14a}$$

and

$$\gamma_t = b_t \frac{w_* \overline{wc}_1}{\overline{w^2} z_i} . \tag{14b}$$

Here C_b and C_t are the mean concentrations of the bottom-up and top-down scalar, $\overline{wc}_0$ is the surface flux of the bottom-up scalar, and $\overline{wc}_1$ is the entrainment flux of the top-down scalar.

The top-down flux budgets given by Moeng and Wyngaard (1984, their Fig. 7), suggest that the turbulent transport and pressure-covariance terms in the top-down flux budgets, i.e., the equivalence of the first and the fourth terms at the rhs of (1) for the top-down scalar, are about the same in most of the PBL. Therefore, we empirically set $b_t = 0$ and consequently $\gamma_t = 0$. For the bottom-up flux budget, the transport term is larger than the pressure term by a factor close to that shown in (4). Thus, we empirically set $b_b = b$ ($\simeq 2$). Note that due to the term γ_b in (13a), our definition of K_b differs from the one in previous studies by Wyngaard and Brost (1984), Moeng and Wyngaard (1984), and Schumann (1989) while the result of (13b) for K_t with $\gamma_t = 0$ is the same.

It appears that the profiles for K_b and K_t can be curve fit as (HM91)

$$\frac{K_b}{w_* z_i} = \left(\frac{z}{z_i} \right)^{4/3} \left(1 - \frac{z}{z_i} \right)^2 \tag{15a}$$

and

$$\frac{K_t}{w_* z_i} = 7 \left(\frac{z}{z_i} \right)^2 \left(1 - \frac{z}{z_i} \right)^3 \tag{15b}$$

for $0 \leq z/z_i \leq 1$. We note that that (15a) is consistent with (12) for $R_H = 0$, and that both (15 a & b) peak at $z/z_i = 0.4$.

Writing

$$\overline{wc} = -K_c\left(\frac{\partial C}{\partial z} - \gamma_c\right), \tag{16}$$

then the eddy diffusivity for any scalar K_c, can be obtained as (see HM91)

$$K_c = \frac{(1 - z/z_i + R_c z/z_i)\, K_b K_t}{(1 - z/z_i)\, K_t + R_c z/z_i K_b}, \tag{17}$$

for $0 \leq z/z_i \leq 1$ and $R_c \geq 0$. Here $R_c \equiv \overline{wc_1}/\overline{wc_0}$ is the entrainment-surface flux ratio of the scalar c. Here we set b_t=0, as mentioned previously.

Unlike the usual K-theory, the eddy diffusivity profile by (17) depends on the ratio of the surface and entrainment fluxes of c. Normalized K_c profiles by (17) are plotted in Fig. 4 for different R_c-ratios (using the parameterized profiles by (15 a & b) as well): $R_c = 0$ retains the *bottom-up* result, and $R_c = 0.5, 1.0, 1.5$ are typical values for entrainment of moisture. For comparison we have also included the *top-down* result ((15b)), which follows from (17) for $R_c \rightarrow \infty$. Overall, it is seen that the entrainment flux can have a significant impact. Typically, K_c increases with increasing values of R_c.

3. LOCAL VERSUS NONLOCAL DIFFUSION IN CCM2

3.1 The local diffusion scheme

Turbulent mixing in global atmospheric models is usually treated by a local vertical diffusion approach. Here we will summarize such an approach, and compare its results with those from the nonlocal approach.

In a local diffusion approach, the turbulent flux is taken to be

$$\overline{w'c'} = -K_c \frac{\partial C}{\partial z}, \tag{((18))}$$

where $c \in (q, \Theta, u, v)$. K_c is an "eddy-diffusivity" for c, which is typically taken as a function of a length scale ℓ_c and local vertical gradients of the mean wind and mean virtual potential temperature, e.g.,

$$K_c = \ell_c^2 S F_c(Ri). \tag{19}$$

Here S is the local shear, defined by

$$S = \left|\frac{\partial V}{\partial z}\right|, \tag{20}$$

and ℓ_c is given by

$$\frac{1}{\ell_c} = \frac{1}{kz} + \frac{1}{\lambda_c}, \tag{21}$$

where again k is Von Karman constant, and λ_c is the so-called asymptotic length scale. Furthermore, $F_c(Ri)$ denotes a functional dependence of K_c on the gradient Richardson number:

$$Ri = \frac{g}{\Theta_v} \frac{\partial \Theta_v / \partial z}{S^2}, \tag{22}$$

where Θ_v is the virtual potential temperature.

There have been a large number of papers dealing with the specification of λ_c and $F_c(Ri)$ (e.g., Blackadar, 1962; Mellor and Yamada, 1974; Louis et al, 1982). In CCM1 (Williamson et al, 1987) $\ell_c = 30$ m was specified, which is thought to be representative for the free atmosphere. Louis et al (1982) distinguish the asymptotic length scales for heat and momentum to be 450 and 150 m, respectively. However, in previous studies a value of 300 m has been used for both heat and momentum. This value seems to be typical for the ABL, but is probably too large for the free atmosphere. Since, there is a lack of atmospheric data to guide us, we took a simple approach, choosing $\lambda_c = 300$ m for $z \leq 1$ km. For larger heights we use a smooth interpolation to a value of 30 m at $z = 10$ km.

For our present implementation of the local K approach, we specify the same stability functions F_c for all variables for simplicity. For unstable conditions ($Ri < 0$) we use

$$F_c(Ri) = (1 - 18Ri)^{1/2} \tag{23a}$$

as in CCM1 (Williamson et al, 1987). For stable conditions ($Ri > 0$) we use (Holtslag and Beljaars,1989):

$$F_c(Ri) = \frac{1}{1 + 10Ri\,(1 + 8Ri)}. \tag{23b}$$

3.2 The nonlocal diffusion scheme

In a nonlocal diffusion scheme the eddy diffusivity depends on characteristic turbulent properties of the ABL, and not on local gradients of mean wind and mean virtual temperature (as in (19)). As we have seen in section 2 for very unstable conditions, the eddy diffusivity depends on the convective velocity scale w_*, the height z, and the height of the ABL z_i. In that case the heat and scalar fluxes are given by (8) and (16), respectively. Besides of nonlocal eddy diffusivities, these expressions incorporate nonlocal countergradient terms. For the wind components no countergradient applies, so (18) is retained. Moreover, in neutral and stable conditions no countergradient correction is of application for any of the variables.

Following Troen and Mahrt (1986) and Holtslag et al (1990), we can write a general form for a nonlocal eddy diffusivity K_c as

$$K_c = k\, w_t\, z \left(1 - \frac{z}{h}\right)^2, \tag{24}$$

where w_t is a turbulent velocity scale and h is now denoting the height of the turbulent boundary layer for all stability conditions. Eq. (24) applies for heat, water vapor and passive scalars. The eddy diffusivity for momentum, K_m, is also defined as (24) but with w_t replaced by another velocity scale w_m. With proper formulation of w_t (or w_m), and h it can be shown that Eq. (24) behaves well from very stable to very unstable conditions in horizontally homogeneous and quasi-stationary conditions. In fact, the turbulent velocity scale depends on height and stability (see the review by Holtslag and Nieuwstadt, 1986). For unstable conditions w_t and w_m are proportional to the so-called convective velocity scale w_*, while for neutral and stable conditions w_t and w_m are proportional to the friction velocity u_*.

For very unstable conditions, (24) can be compared with (12). It appears that the formulations are very similar, allthough (24) does not fullfil the free convection limit of the surface layer and that it is independent of the entrainment ratio. For simplicity we will retain (24) here. Moreover, for scalar transport the eddy diffusivity may depend on the transported scalar as formulated by (17). Since the latter proposals need further elaboration, we will make the usual assumption that the eddy diffusivity for specific humidity is similar to the one for heat.

We note that Eq. (24) is very similar to the one proposed by Brost and Wyngaard (1978) for the stable boundary layer. The cubic shape of (24) is consistent with the eddy-diffusivity profile originally proposed by O'Brien (1970), which he derived on basis of the physical requirements that the profile and its first derivative be continuous with height and match to surface layer similarity. The advantage of the present approach over the local eddy diffusivity approach by (19), is that large eddy transport in the ABL is accounted for in the very unstable case. Above the ABL, $\gamma_c = 0$ so (16) reduces to (18) with K_c given by (19). In that case we use $l_c = 30$ m. Near the top of the ABL we use the maximum of the values by (19) and (24) although (24) almost always gives the larger value in practice (except in the very stable case).

The countergradient terms of (8) and (16), represents nonlocal influences on the mixing by turbulence. As such, this term is small in stable conditions, and is therefore neglected in these conditions. For unstable conditions, however, most transport of heat and moisture is done by turbulent eddies with sizes on the order of the depth h of the ABL. In such cases, a formulation for γ_c consistent with the eddy formulation of (24) is given by

$$\gamma_c = a\frac{w_*(\overline{w'c'})_0}{{w_m}^2 h} \quad , \tag{25}$$

where a is a constant ($a = 7.2$, see HB92) and $(\overline{w'c'})_0$ is the surface flux (in kinematic units) of the transported scalar, which may be water vapor or potential temperature. No countergradient term applies for momentum, as noted above. The countergradient correction van-

ishes under neutral conditions, for which $w_* = 0$. The latter property is desirable, and was not apparent in the original form for γ_c by Troen and Mahrt (1986).

The formulations of the eddy-diffusivity and the countergradient terms are dependent on the boundary layer height h. Here we follow the procedures in Troen and Mahrt (1986) and Holtslag et al (1990) for the determination of h.

3.3 CCM2 model description and experiments

To show the impact of local versus nonlocal diffusion, HB92 used the latest version of the NCAR community climate model (CCM2). Although CCM2 is an outgrowth of the previous version (CCM1), described by Williamson et al. (1987), the model has been revised so extensively that only a few papers documenting the previous version are still relevant. The vertical coordinate, numerical approximations, and most physical parameterizations have been replaced, as summarized briefly by Kiehl(1991) and HB92. Detailed descriptions of changes to the model outside of the ABL scheme are beyond the scope of this paper and will be discussed in a number of forthcoming papers, most of which are still in preparation. We summarize some of the physical parametrizations here.

The short wave radiation parameterization (Briegleb, 1992) now uses the δ-Eddington method and incorporates both diurnal and annual cycles of insolation. The long wave radiation parameterization has also been updated (principally affecting the upper stratosphere). The cloud fraction parameterization used for radiative purposes is a generalization of the method proposed by Slingo (1987). The diagnosed cloud fraction depends on relative humidity, vertical motion, static stability and precipitation rate. Once clouds appear, their liquid water concentration is specified as function of latitude and height for the radiation calculations (similar to the description in Kiehl 1991).

Land temperatures are predicted using a diffusion equation for the surface and 3 subsurface layers with differing heat capacities. Sea surface temperatures are prescribed by linear interpolation between climatological monthly mean values from Shea et al (1990). The surface fluxes are calculated with the usual transfer coefficients between the surface and the first model level (e.g., Beljaars and Holtslag 1991). Compared to CCM1 we have updated the stability dependence of the transfer coefficients, according to Holtslag and Beljaars (1989). In the ABL, CCM2 incorporates the nonlocal diffusion scheme (see section 3.2). A simple mass flux scheme (Hack 1992) is used to represent both deep and shallow convection. The mass flux scheme utilizes turbulent temperature and moisture perturbations, which are provided by the nonlocal ABL scheme. As such, there is a direct coupling between the surface fluxes and the convection parametrization.

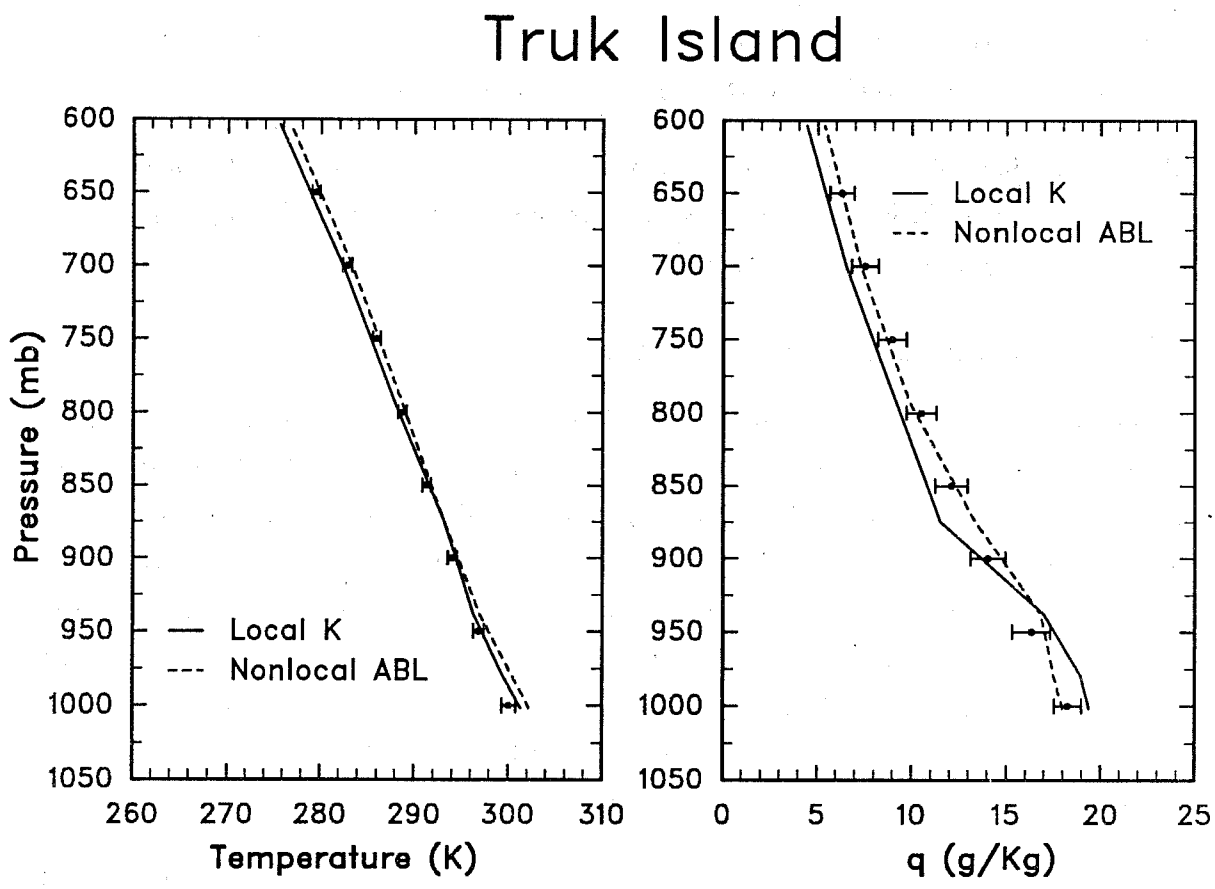

Figure 5. The simulated mean temperature (left panel) and specific humidity profile (right panel) for July in a gridpoint near Truk Island (7.5 °N,151°E), in comparison with radiosonde observations (dots with error bars). Solid lines reflect results with CCM2 using the local diffusion scheme, and dashed lines refer to CCM2 with the nonlocal diffusion scheme.

A decadal integration of a test version of CCM2 was used as the starting point for the two experiments discussed here. The results presented below were obtained from two 60 day integrations of the model, beginning on June 2 of the seventh year of the decadal integration. In the first experiment, the ABL scheme was updated slightly (to that described above) from the scheme used in the decadal integration. In the second experiment, the ABL scheme was replaced by the local K scheme. In all of the above experiments, the dry adiabatic procedure was not used (except in the top three model layers). The results shown below are 31 day averages for July. The land surface temperatures in the second (local K) experiment are probably not yet in equilibrium, however, we will concentrate on results over ocean points.

The observations, used to compare against the model results, were obtained by taking the monthly averages of daily radiosonde reports of temperature and dew point depression from US Control Sources. Dew point depressions were converted to specific humidities prior to averaging. The profiles show the July mean averaged over all available years (from 15 to $>$ 40 years depending on the station) and the standard deviation (interannual variability) of the monthly means. Comparison data from the model is taken by averaging all grid points with $\pm 3°$ of the station.

3.4 Comparison within CCM2

Fig. 5 shows the observed July mean vertical profiles of temperature and specific humidity of Truk Island (7.5 °N, 151 °E) in the tropics, compared to the simulated profiles produced using the local K approach (experiment 2; solid lines) and the nonlocal approach (experiment 1; dashed lines). Remember that over the oceans the sea surface temperature is prescribed. It is seen that in particular the vertical structure of the specific humidity profile is much better simulated with the nonlocal ABL scheme. With the local scheme the total mixing of specific humidity is underestimated, resulting in the atmospheric levels near the surface becoming too moist. This will directly affect the surface fluxes of latent and sensible heat and may result in unrealistically large amounts of clouds at low levels. The fact that the temperature and specific humidity profiles are also influenced at heights above the ABL is due to the interaction of the nonlocal scheme with other parts of the model.

Figure 6 shows the temperature and specific humidity profiles obtained with the two model integrations using the nonlocal (experiment 1) and local diffusion schemes (experiment 2), respectively. The comparison is now made for the ocean gridpoint near the Azores (38.7 °N, 27.1 °W), for which we have also shown the mean obseved profile. We note that the results with the two diffusion schemes are quite different. The temperature profile for the Azores is very well represented with the nonlocal scheme. The specific humidity profile, however, seems

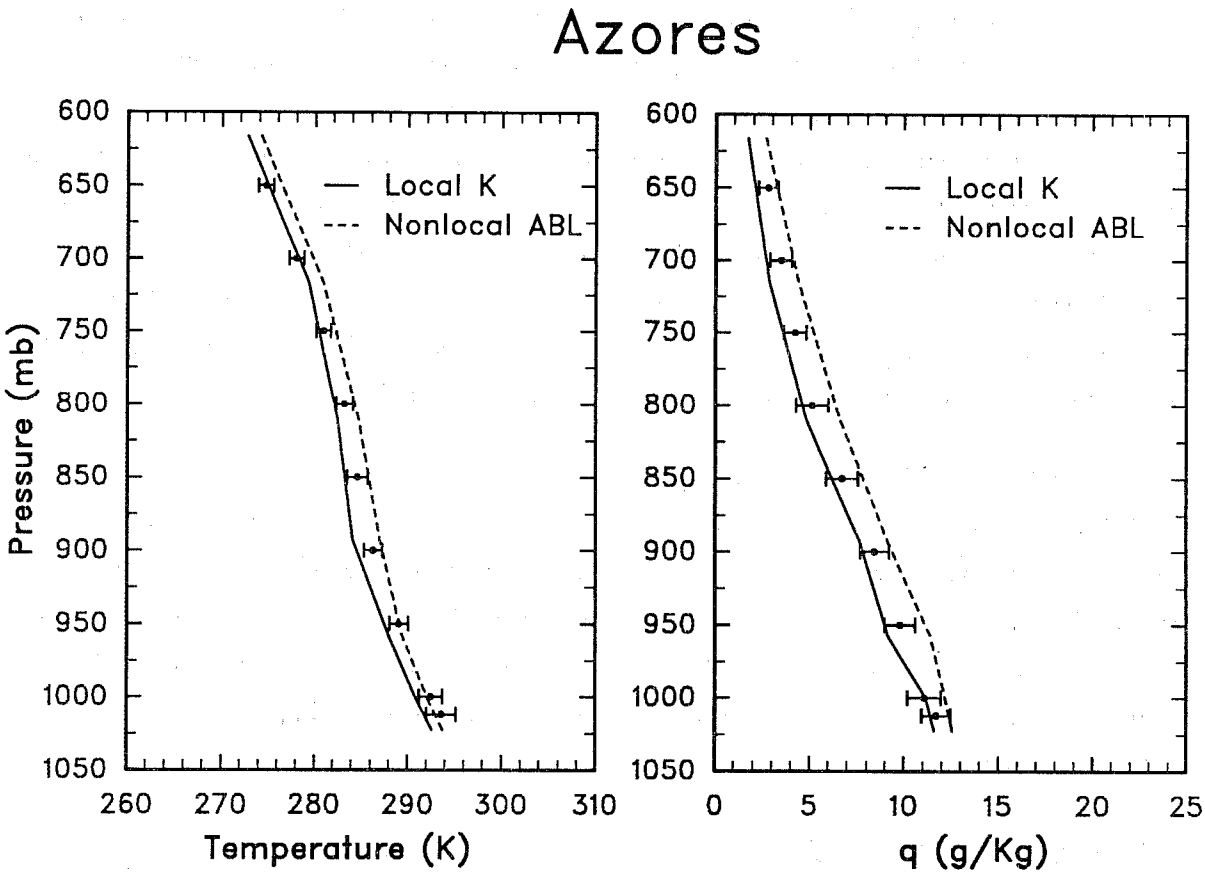

Figure 6. The simulated mean temperature (left panel) and specific humidity profile (right panel) for July in a gridpoint near the Azores (38.7 °N, 27.1 °W), in comparison with radiosonde observations (dots with error bars). Solid lines reflect results with CCM2 using the local diffusion scheme, and dashed lines refer to CCM2 with the nonlocal diffusion scheme.

to be too moist using the nonlocal scheme and too dry using the local scheme (except near the surface).

The fair agreement of the results by the nonlocal scheme with the observations is explained by the fact that the nonlocal scheme is a better description of the physics, and that this scheme is able to represent entrainment effects near the top of the ABL. The results with the local scheme indicate too less vertical distribution of heat and moisture. This is due to the lack of entrainment, and due to the local description of vertical exchange. However, for locations in which deep convection is important, the outputs of the runs with the two vertical diffusion schemes are very similar (not shown).

The overall effect of replacing the nonlocal ABL scheme with the local K scheme is summarized in Figures 7, 8, and 9. These figures show the differences in the zonal mean temperatures, specific humidities, and areal extent of cloudiness, respectively. The lower part of the troposphere is warmer in the nonlocal ABL case throughout the tropics and middle latitudes. This change is almost certainly significant, although the experiments are too short for statistical testing. The specific humidity shows the difference anticipated from the individual profiles and the tendencies. The nonlocal ABL scheme dries the lowest model levels and moistens near 850 mb relative to the local K scheme.

The nonlocal scheme utilizes countergradient effects for heat and moisture. From sensitivity studies with the model, we obtained that a factor of two variation in magnitude of the countergradient terms has only minor influence on the simulations. However, when the countergradient terms are removed there is a significant impact. Neglecting these terms, the nonlocal scheme produces lower boundary layer heights and therefore smaller values for the diffusivities. Consequently, the entrainment at the top of the ABL is underestimated.

There are several important consequences for the rest of the model which follow from the upward shift in the water distribution between the nonlocal ABL and the local K cases. There are direct impacts both on the convection and on the clear sky radiative processes. There is also a significant change in the distribution of low clouds. Although the net cloud amount below 700 mb is similar in the two cases, the clouds are shifted upward in the nonlocal ABL case (Fig. 9). Very low clouds, which tend to form in the bottom two model levels with a local K scheme, are virtually eliminated by the nonlocal ABL scheme. This results in a more realistic cloud distribution.

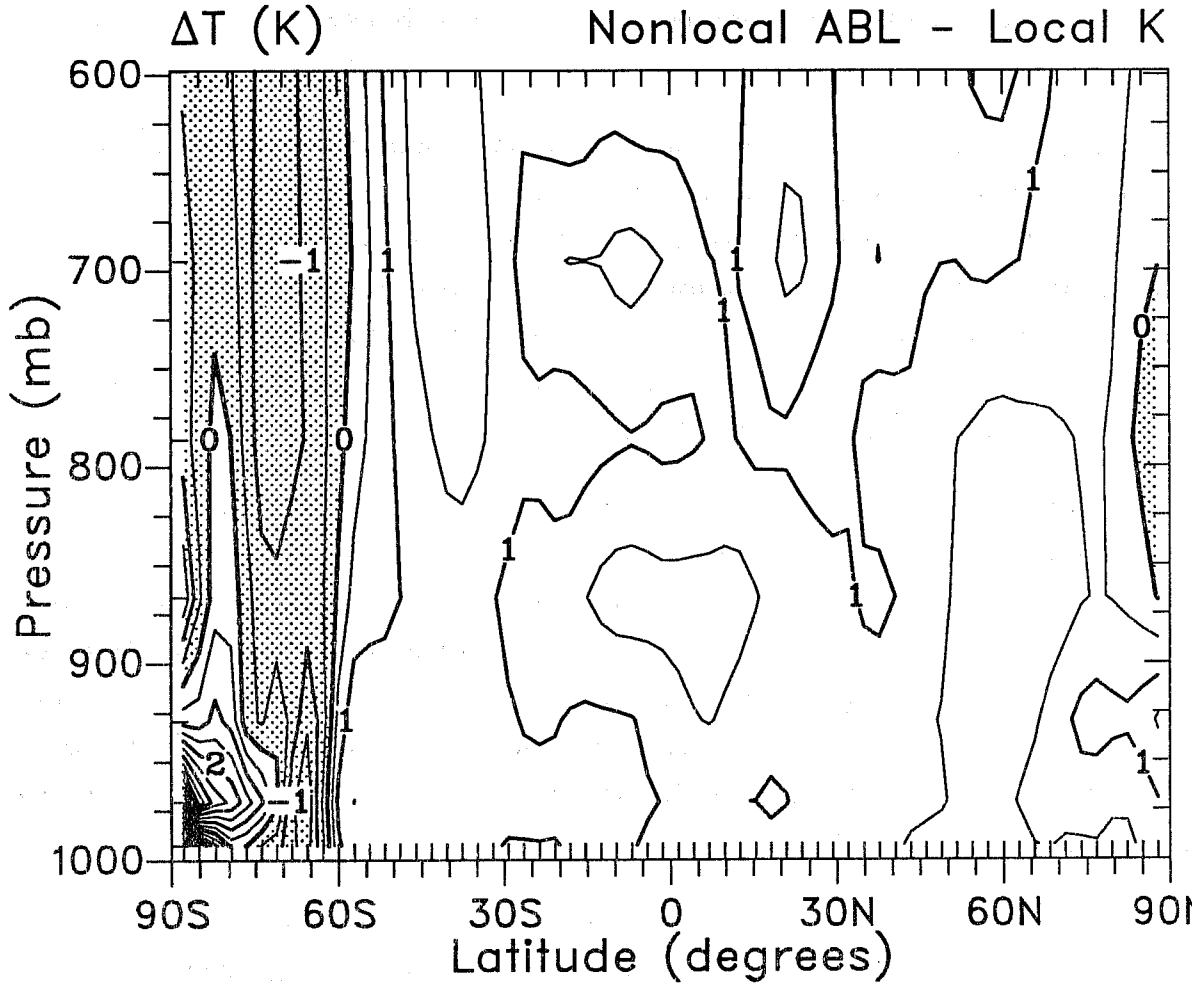

Figure 7 The zonal mean temperature (T) differences between the simulations with the non-local and local diffusion schemes versus pressure. Results are for July, and contours are plotted from -2.5 K to 5.5 K with a interval of .5 K.

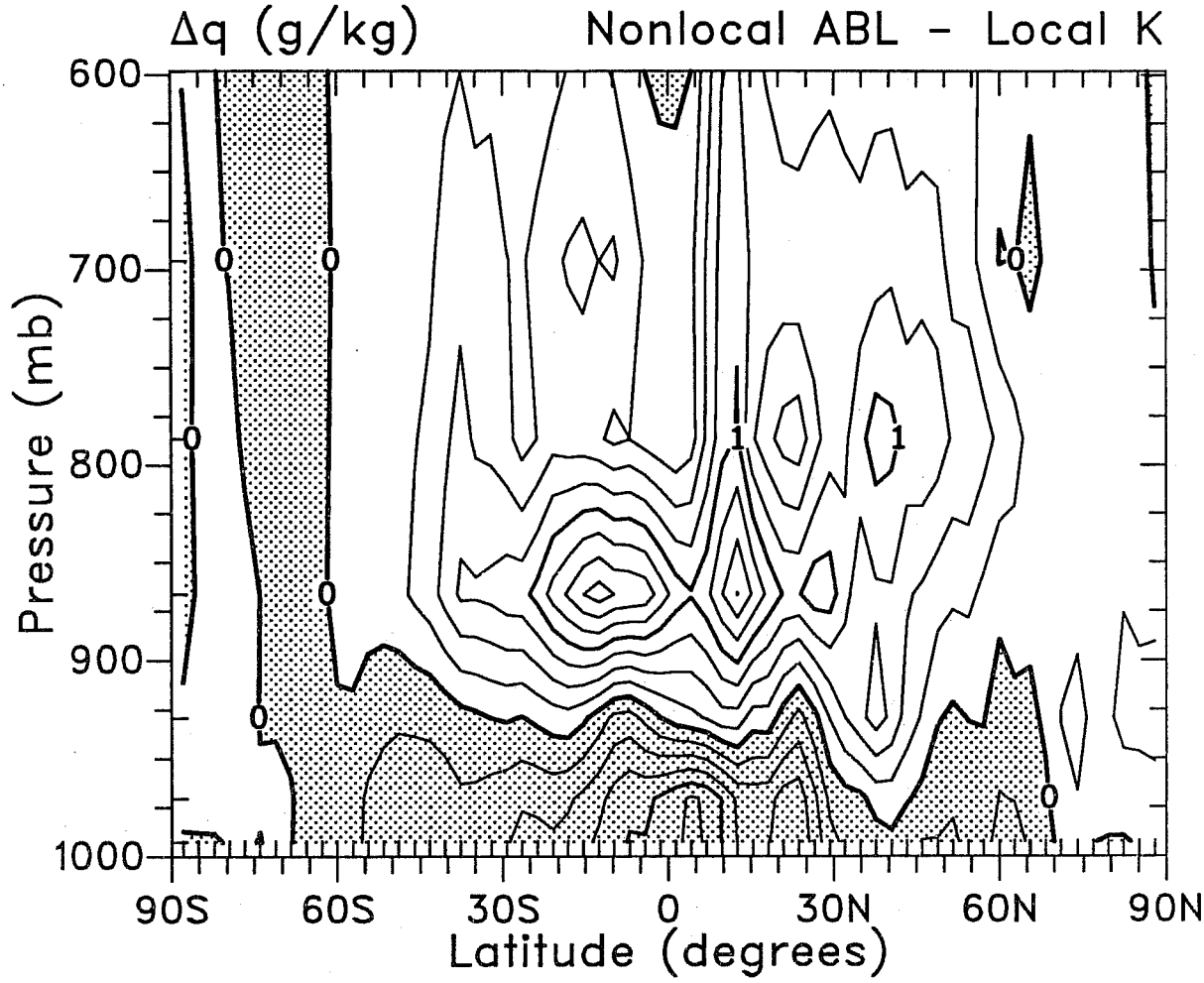

Figure 8. Similar as Figure 7, but for specific humidity (q). The contours are given from -1.25 g/kg to 1.75 g/kg with a interval of .25 g/kg.

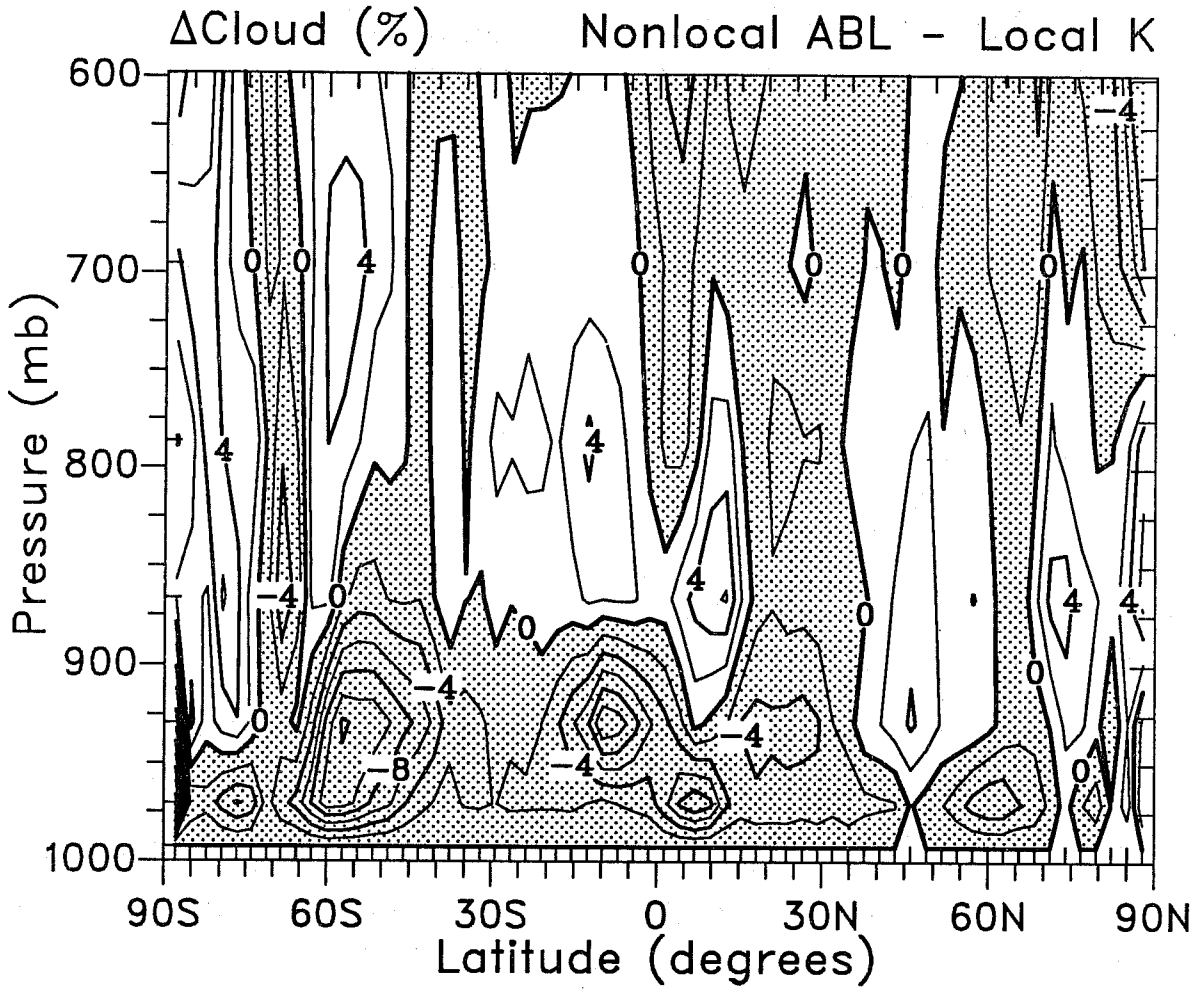

Figure 9. Similar as Figure 7, but for cloud fraction. Contours are from −14% to 8% with a interval of 2%.

4. SUMMARY AND DISCUSSION

In section 2 of this paper we summarize recent findings for the vertical exchange of heat and scalars in the convective, atmospheric boundary layer (Holtslag and Moeng, 1991). Such a boundary layer is dominated by fast rising updrafts and slower descending downdrafts, and by large-eddy nonlocal turbulent transport. To describe this nonlocal transport in the stationary, horizontally-homogeneous CABL, parametrizations are given for the pressure-covariance terms (P) and the transport terms (T) in the heat-flux equation and in the flux equations for the top-down and bottom-up scalars. This leads directly to (modified) descriptions for counter-gradient terms in the flux-gradient approach. As such, the work by Deardorff (1972) is extended. The outcome of the present parametrizations, is physically appealing and consistent with previous independent derivations (Priestley and Swinbank 1947; Wyngaard and Weil 1991). The findings are written in a modified flux-gradient approach, with a nonlocal diffusivity and countergradient correction for heat and scalars. As such, the findings are a generalization of those by Troen and Mahrt (1986).

In section 3 of this paper we have summarized the work by Holtslag and Boville (1992), who studied the impact of two schemes for vertical boundary-layer diffusion within the context of the Community Climate Model, version 2 (CCM2). Among other things, the two schemes differ in their specification of the eddy-diffusivity, which can be regarded as a local versus a nonlocal formulation. The outputs of the local and nonlocal diffusion schemes have been shown in comparison with radiosonde observations for two ocean locations. The impact of the two diffusion schemes within CCM2 is illustrated with zonal mean difference plots for temperature, specific humidity, and low level cloud fraction.

Generally, the nonlocal scheme provides more realistic temperature and moisture profiles. The differences due to the two diffusion schemes in low-level zonal mean temperature and specific humidity are typically 1 K and 1 g/kg, respectively. As a result, the low clouds are shifted upward from the lowest two model levels to near 850 mb in the tropics.

Future studies may focus on the interaction of the nonlocal diffusion scheme with the hydrological cycle, e.g. deep and shallow convection, and the land surface parameterization. Special consideration may be given to the influence of entrainment on the performance of the nonlocal scheme.

Aknowledgments We thank our colleagues at KNMI and NCAR for useful comments and discussions. This work was initiated during a longtime visit of the first author to NCAR, for which he aknowledges financial support. The National Center for Atmospheric Research is sponsored by the National Science Foundation.

REFERENCES

Adrian, R.J., R.T.D.S. Ferreira, and T. Boberg,1986: A review of turbulent thermal convection in wide horizontal fluid layers. *Exper. in Fluids*, **4**, 121–141.

Beljaars, A. C. M., and A. A. M. Holtslag, 1991: Flux parameterization over land surfaces for atmospheric models. *J. Appl. Meteorol.*, , **30**, 327–341.

Blackadar, A. K., 1962: The vertical distribution of wind and turbulent exchange in neutral atmosphere. *J. Geophys. Res.***67**, 3095–3103.

Briegleb, B. P., 1992: Delta-Eddington approximation for solar radiation in the NCAR Community Climate Model. *J. Geophys. Res.*(under review).

Brost, R. and J. C. Wyngaard, 1978: A model study of the stably-stratified planetary boundary layer. *J. Atmos. Sci.*, **35**, 1427-1440.

Crow, S.C., 1968: Visco-elastic properties of fine-grained incompressibble turbulence. *J. Fluid Mech.*, **33**, 1–20.

Deardorff, J.W., 1966: The counter-gradient heat flux in the lower atmosphere and in the laboratory. *J. Atmos. Sci.*, **23**, 503–506.

Deardorff, J. W., 1972: Theoretical expression for the countergradient vertical heat flux. *J. Geophys. Res.*, **77**, 5900-5904.

Ebert, E.E., U. Schumann, R.B. Stull, 1989: Nonlocal turbulent mixing in the convective boundary layer evaluated from large-eddy simulation. *J. Atmos. Sci.*, , bf 46, 2178–2207.

Hack, J. J., 1992: Parameterization of moist convection in the NCAR Community Climate Model, CCM2 (in preparation).

Holtslag, A.A.M. and F.T.M. Nieuwstadt, 1986: Scaling the atmospheric boundary layer. *Boundary-Layer Meteor.*, **36**, 201–209.

Holtslag, A. A. M. and A. C. M. Beljaars, 1989: Surface flux parameterization schemes: Developments and experiences at KNMI. Proceedings of the ECMWF workshop on Parameterization of fluxes over land surface, ECMWF Reading UK, 121–147 (Also available as KNMI Sci. Rep. 88–06, De Bilt NL, 27p.).

Holtslag, A. A. M., E. I. F. de Bruijn, H.-L. Pan, 1990: A high resolution air mass transformation model for short-range weather forecasting. *M. Wea. Rev.*, **118**, 1561–1575.

Holtslag, A. A. M. and C.-H. Moeng, 1991: Eddy diffusivity and countergradient transport in the convective atmospheric boundary layer. *J. Atmos. Sci.*, , **48**, 1690–1698.

Holtslag, A.A.M. and B.A. Boville, 1992: Local versus nonlocal boundary-layer diffusion in a global climate model. *Submitted.*

Kiehl, J. T., 1991: Modelling and validation of clouds and radiation in the NCAR Community Climate Model (CCM2). Proceedings of the ECMWF/WCRP Workshop on Clouds, Radiative Transfer and the Hydrologic Cycle, ECMWF, Reading UK, 249–272.

Lenschow, D.H., J.C. Wyngaard, and W.T. Pennell, 1980: Mean-field and second- moment budgets in a baroclinic, convective boundary layer. *J. Atmos. Sci.*, **37**, 1313–1326.

Louis, J.F., 1979: A parametric model of vertical eddy fluxes in the atmosphere. *Bound.-Layer Meteorol.*, **17**, 187–202.

Louis, J. F., M. Tiedtke, and J. F. Geleyn, 1982: A short history of the PBL parameterization at ECMWF. Proceedings of the ECMWF workshop on Boundary-Layer Parameterization, ECMWF, Reading, UK, 59–79.

Mellor, G. L., and T. Yamada, 1974: A hierarchy of turbulence closure models for planetary boundary layers. *J. Atmos. Sci.*, , **31**, 1791–1806.

Moeng, C.-H., and J.C. Wyngaard, 1984: Statistics of conservative scalars in the convective boundary layer. *J. Atmos. Sci.*, **41**, 3161–3169.

Moeng, C.-H., and J.C. Wyngaard, 1986: An analysis of closures for pressure-scalar covariances in the convective boundary layer. *J. Atmos. Sci.*, **43**, 2499–2513.

Moeng, C.-H., and J.C. Wyngaard, 1989: Evaluation of turbulent transport and dissipation closures in second-order modeling. *J. Atmos. Sci.*, **46**, 2311–2330.

Nieuwstadt, F.T.M., 1984: Some aspects of the turbulent stable boundary layer. *Boundary-Layer Meteor.*, **30**, 31–55.

O'Brien, J.J., 1970: A note on the vertical structure of the eddy exchange coefficient in the planetary boundary layer. *J. Atmos. Sci.*, **27**, 1213-1215.

Panofsky, H.A., and J.A. Dutton, 1984: Atmospheric Turbulence; Models and methods for engineering applications. Wiley, New York, 397p.

Priestley, C.H.B. and W.C. Swinbank, 1947: Vertical transport of heat by turbulence in the atmosphere. *Proc. Roy. Soc.*, **A189**, 543–561.

Schumann, U., 1987: The counter-gradient heat flux in turbulent stratified flows. *Nuclear Engineering and Design*, **100**, 255–262.

Schumann, U., 1989: Large-eddy simulation of turbulent diffusion with chemical reactions in the convective boundary layer. *Atmospheric Environment*, **23**, 1713–1727.

Shea, D. J., K. E. Trenberth, R. W. Reynolds, 1990: A global monthly sea surface temperature climatology. NCAR Techn. Note NCAR/TN-345+STR, Boulder CO, 167p.

Slingo, J. M., 1987: The development and verification of a cloud prediction scheme for the ECMWF model. *Quart. J. Roy. Meteor. Soc.*, , **113**, 899–927.

Troen, I. and L. Mahrt, 1986: A simple model of the atmospheric boundary layer; Sensitivity to surface evaporation. *Boundary-Layer Meteor.*, **37**, 129–148.

Williamson, D. L., J. T. Kiehl, V. Ramanathan, R. E. Dickinson, and J.J. Hack, 1987: Description of NCAR Community Climate Model (CCM1), NCAR Tech. Note, NCAR/TN–285+STR, National Center for Atmospheric Research Boulder, Colo. 112 pp.

Wyngaard, J.C., 1987: A physical mechanism for the asymmetry in top-down and bottom-up diffusion. *J. Atmos. Sci.*, **44**, 1083–1087.

Wyngaard, J.C. and R.A. Brost, 1984: Top-down and bottom-up diffusion of a scalar in the convective boundary layer. *J. Atmos. Sci.*, **41**, 102–112.

Wyngaard, J.C. and J.C. Weil, 1991: Transport asymmetry in skewed turbulence. *Physics of Fluids A*, **3**, 155–162.